

DETERMINATION OF CALCIUM IN WATER SAMPLES BY USING Au-ELECTRODE IN HCl SOLUTION IN THE ABSENCE AND PRESENCE OF A CRYSTAL VIOLET AND ENVIRONMENTAL STUDIES

Safa Q. Hussien*, Mohamed M. El-Defrawy, Esam A. Gomaa and Marwa G. El-Ghalban

Chemistry Department, Faculty of Science, Mansoura University, Mansoura, Egypt

(Received May 15, 2023; Revised October 2, 2023; Accepted October 12, 2023)

ABSTRACT. The hydrochloric acid (HCl 0.1 M) supporting electrolyte was used in the electrochemical estimation cyclic voltammetry for CaCl_2 concentrations also using crystal violet dye or (hexamethyl pararosaniline) as ligand. For oxidation and reduction waves, the potential range is 0.5 V, -0.5 V. The interaction of calcium ions with crystal violet was examined using several analytical estimates, and kinetic and thermodynamic parameters. The analytical concentration for calcium ions in different samples especially in Nile River were estimated in the range from 1.6 to 14.3 mmol. The estimation of calcium ion concentrations was achieved up to 11.49 mmol in waste water in Mansoura University. Applications were made for calcium estimation of different water samples and molecular docking of the calcium-crystal violet complex against the Hepatitis C viral proteins (4i33, 4KTC), roving strong bonds of interaction were observed. And anti-bacterial effect on calcium complex with crystal violet and face mask N-95 tissue.

KEY WORDS: Calcium ions, Thermodynamic properties, Solvation parameters, Nile water samples, Anti-bacterial, Molecular docking

INTRODUCTION

All living things, including humans, require calcium to survive. Calcium is the most prevalent element in the body and is essential for bone health. Calcium is necessary for humans to develop healthy teeth and strong skeletons, and to move their muscles and maintain their cardiovascular systems. Ca^{2+} ions can cause problems with the muscles and bones, blood clotting, death, kidney stones, and irregular enzyme activity. The benefits of cyclic voltammetry include its clarity, simplicity, low cost, and speed. The main focus of this work is on estimating the calcium ions in electrolytes that support HCl in both the absence and presence of crystal violet. Unfortunately, wastewater treatment systems are frequently unable to entirely remove commercial dyestuffs, and as a result, they are detected in soil and river sediment as a result of chemical waste disposal. The dye has been used extensively in human and veterinary medicine as a biological stain and textile dye [1-3]. Water hardness is an important parameter of water quality and from this depends on water use in many industrial branches; it depends on the presence of Mg and Ca ions at the same time present the sum of carbonate and noncarbonated. The Ca in concentration in the water of the river is 32-50 mg/L, a water sample was taken directly from the Nile River in Mansoura city near the university. This sample was filtered only to remove the solid deposits. Analysis of the calcium ions was done by taking different additions and applying the previous method for analysis and estimation in the absence and presence of crystal violet in 0.1 M HCl medium and using working electrode gold 18 karat [4]. Historically significant as a topical antiseptic, crystal violet also contains antibacterial, antifungal, and anthelmintic effects. Modern medications have essentially replaced the dye's usage in medicine. Gentian violet is frequently used in body piercing, especially surface surface piercings. Marking blue, which is made of methylated spirits, shellac, and gentian violet, is used to mark out components in metalworking [5, 6].

*Corresponding author. E-mail: safakasim83@yahoo.com

This work is licensed under the Creative Commons Attribution 4.0 International License

EXPERIMENTAL

Chemicals

The substances employed (calcium chloride, hydrochloric acid, and crystal violet) were obtained from Sigma-Aldrich. A 0.1 M HCl was prepared from El Gomheria Company hydrogen HCl. The three electrodes used in the DY2000 (USA) system for the cyclic voltammetry measurements are the working electrode (gold electrode), the reference electrode (Ag/AgCl/saturated KCl), and the auxiliary electrode (Pt electrode) [7, 8].

Preparation of the face mask

We obtained two different kinds of medical masks from the pharmacy, one type N-95 and the other regular. We then cut the masks into 1 x 1 cm pieces, prepared a calcium chloride and crystal violet dye solution at a concentration of 0.1 M each, and soaked the mask pieces in the solution for an hour to absorb it. The combination was exposed to IR light, and after drying, it was cultivated in a lab at the Mansoura University Faculty of Science.

Preparation of the waters samples

The water sample was obtained directly from the Nile River in Mansoura City, close to Mansoura University in Egypt, and the wastewater sample was obtained from the same location in Mansoura city. Both samples were filtered using filter paper before analysis.

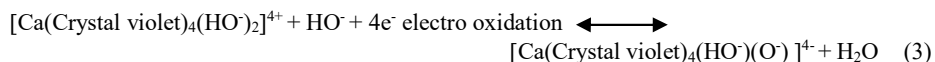
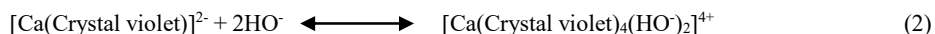
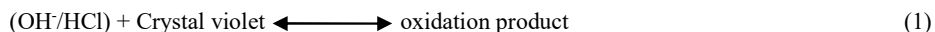
RESULTS AND DISCUSSION

Calcium ion determination

The cyclic voltammetry determination in 0.1 M HCl solution, and adding different calcium chloride (0.1 M) using gold electrode the preparation of 18-karat working electrode was explained in previous work. The waves in the presence of gold electrode at 0 V, -0.25 V and -0.5 V and two reduction waves at -0.25 V and -0.5 V. Oxidation peak may be proceeding using the equations in reference [9]. This peak is sensitive for the calcium ion evaluation analytically [10-14]. Different straight lines are obtained explained proving the diffusion controlled reaction.

Effect of Ca²⁺ in the presence of crystal violet

The peaks for the oxidation reactions occurred at +0.25 and +0.5 V are explained as equations in reference [9]. In presence of calcium alone or calcium plus crystal violet following reactions occurred:



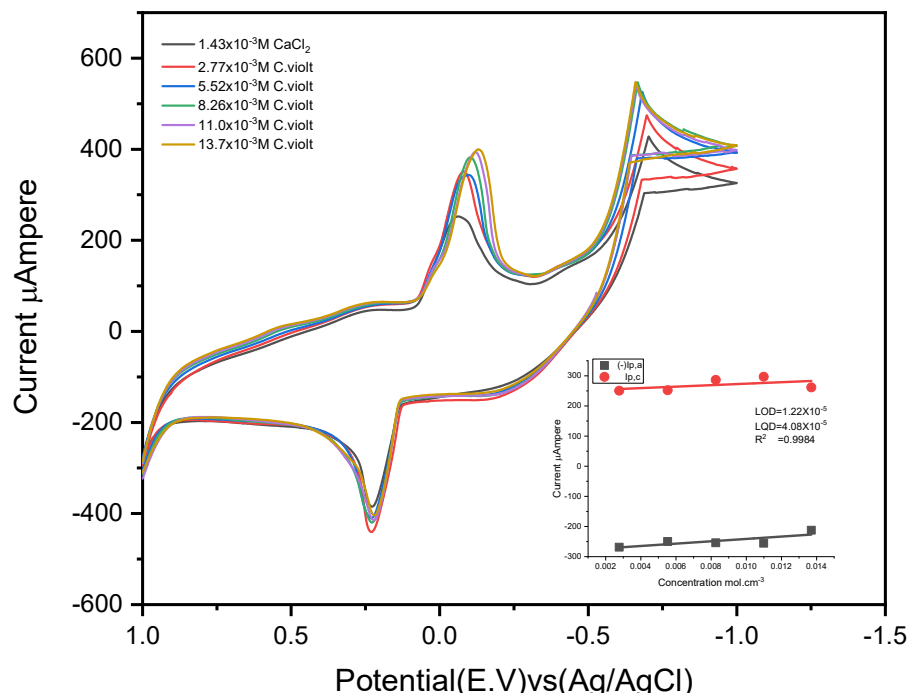


Figure 1. Voltammograms for (1.43×10^{-3} M) CaCl_2 and effect of crystal violet on it in hydrochloric acid medium (0.1 V/s, 291.15 K).

The voltammogram contains many evaluated data and R^2 have approximately constant value [15-18]. Most of the statistics in Table 1 are reduced by an increase in the ligand concentration. Adsorption electrical parameters Γ_a , Γ_c and Q_a are decreased clearly by decrease in ligand concentration favoring complexation reaction.

Effect of calcium ion scan rate in presence crystal violet

All the analysis data following references [19-21] are seen in the previous table.

Limit of detection (LOD) of calcium ion in presence and absence of crystal violet

The LOD for Ca^{2+} ions and crystal violet were 9.69×10^{-3} and 4.08×10^{-5} M, respectively. The evaluated values for the LOD were (2.9×10^{-3} and 1.22×10^{-5} M) [22-26].

Applications

Calcium analysis in Mansoura Nile river water

The Ca ion concentration in the water of the river was 32-50 mg/L. Water sample was taken directly from the Nile River in Mansoura city near the university. This sample was filtered only to remove the solid deposits. Analysis of the calcium ions was done by taking different additions and applying the previous method for analysis and estimation in the absence and presence of crystal violet in 0.1 M HCl medium and using working electrode gold 18-karat. The appearance

of three different waves is given in Figure 2, wave (1) is the reduction wave of Ca^{2+} , wave (2) is the oxidation wave of Ca^{2+} , wave (3) is the O_2 wave that catalytically happened in the presence of Ca^{2+} as the decomposition of water through the equation [27, 28]:



The concentration of calcium ions in the water of the Nile River was determined by the atomic absorption spectrophotometer, the value was 1 ppm.

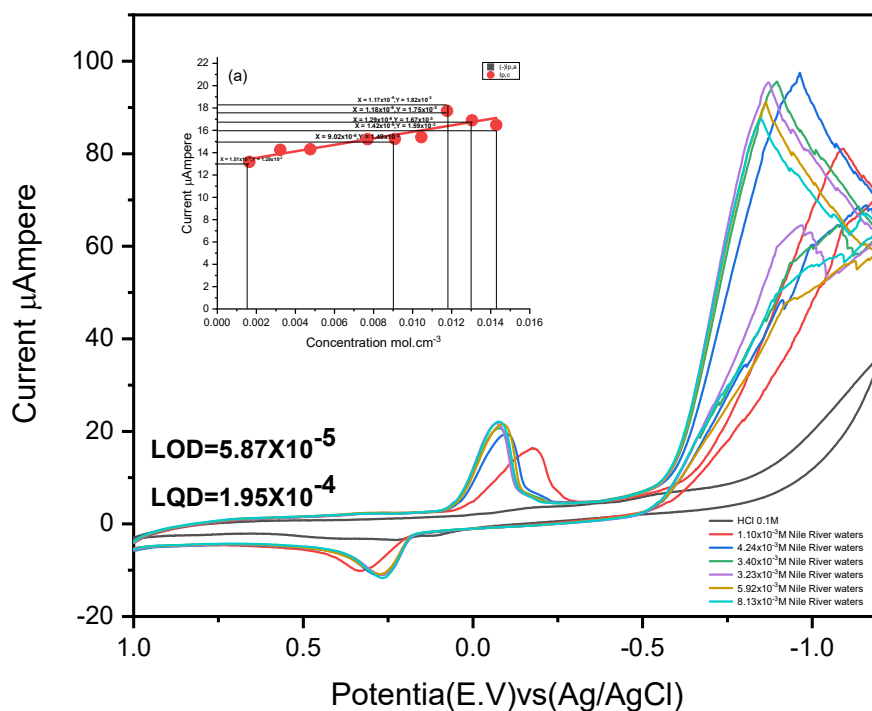


Figure 2. Nile River calcium ions concentrations in the used supporting electrolyte (0.1 V/s and 291.15 K). (a) Values of I_p , a versus calcium ion concentrations.

Table 1. Calcium ion parameters in Nile River (0.1 V/s, 291.15 K).

[M] x10 ³ mol.L ⁻¹	Volt			Amp		$I_{p,a}/I_{p,c}$	Volt E°	R ²
	(-) Ep,a	Ep,c	ΔEp	(-)Ip,ax10 ⁶ mAmp	Ip,cx10 ⁶ mAmp			
1.10	0.3166	0.1686	0.4852	75.3	12.9	0.5858	0.0739	0.9985
4.24	0.2610	0.0726	0.3336	82.3	14.9	0.5533	0.0941	0.9725
3.40	0.2600	0.0762	0.3363	81.8	17.4	0.4701	0.0918	0.9764
3.23	0.2422	0.0447	0.2869	79.4	16.7	0.4743	0.0987	0.9755
5.92	0.2701	0.0893	0.3595	80.6	19.1	0.4221	0.0903	0.9785
8.13	0.2556	0.0430	0.2987	90.3	16.0	0.5645	0.1063	0.9744

$D_{ax}10^5$ $cm^2 \cdot S^{-1}$	$D_{cx}10^5$ $cm^2 \cdot S^{-1}$	$E_{pc/2}$	$E_{pa}-E_{pc/2}$	$\alpha n a$	$k_{sc} \times 10^2$	$\Gamma_{cx}10^9$ Mol/cm	$(+)Q_{cx}10^5$ coulomb	$\Gamma_{ax}10^9$ mol/cm	$(-)Q_{ax}10^5$ coulomb
8.96	6.7996	0.0653	0.1033	0.4509	3.15	1.0644	6.45	6.2367	3.78
2.54	2.0409	0.0123	0.0603	0.7725	6.04	1.2313	7.46	6.8132	4.13
3.14	2.9718	0.0031	0.0731	0.6367	8.42	1.4399	8.73	6.7697	4.10
3.22	3.0188	0.0031	0.0416	1.1197	4.24	1.3867	8.40	6.5782	3.99
1.78	1.8735	0.0131	0.0762	0.6112	8.25	1.5805	9.58	6.672	4.04
1.45	1.1446	0.0018	0.0449	1.0365	1.95	1.3243	8.02	7.4772	4.53

Analysis of the main calcium peak in Figure 2 was done and the evaluated data are given in Table 1. A slight increase in analysis value was increased by adding River Nile water quantities indicating a diffusion mechanism. Catalytic O_2 peak (peak 3) was observed [29, 30]. Applying the anodic peak (peak 2), we can estimate the calcium ion concentration as shown in Figure 2A, we can estimate calcium ion concentration in the Nile River either following the anodic or cathode peak. Increasing volume of the Nile River quantity supporting the diffusion mechanism [31, 32].

Calcium analysis in Nile River in presence of crystal violet

Different addition of crystal violet was studied in cyclic voltammetry in 0.1 M HCl and using an Au 18-Karat working electrode Figure 3 and Table 2 gave the analytical obtained data showing a decrease in most data proving the complexation between crystal violet and calcium in the Nile River.

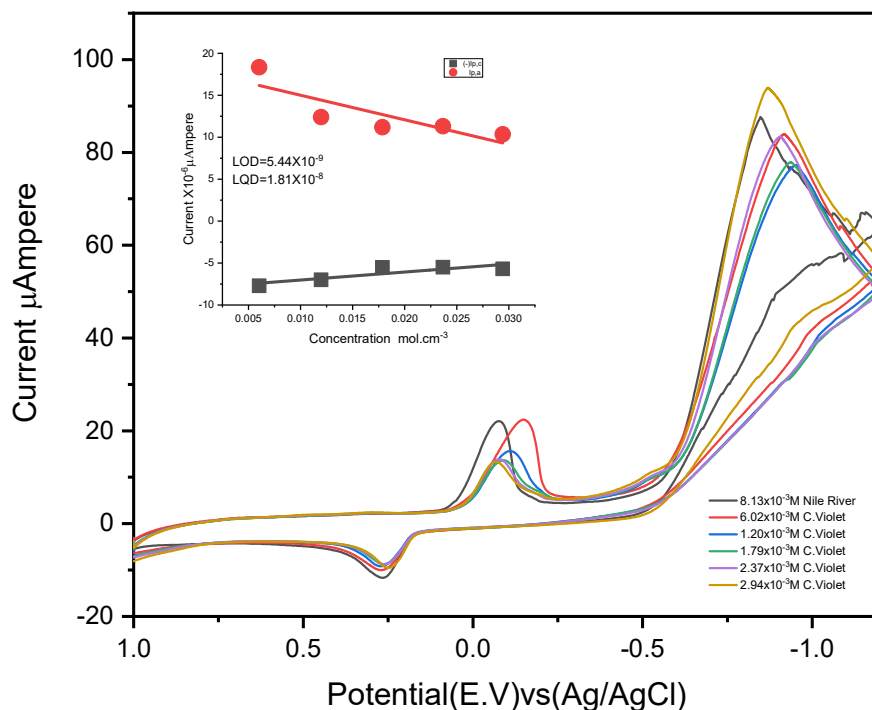


Figure 3. Crystal violet effect for calcium ions in HCl for Nile water sample at scan velocity (0.1 V/s and 291.15 K).

Table 2. Crystal Violet effect on (8.13×10^{-3} M) calcium ions of Nile River by using 0.1 M HCl (0.1 V/s and 291.15 K).

Volt			Amp		Ip,a/Ip,c	E°	[L]x10 ³ mol.L ⁻¹
Ep,a	Ep,c	ΔEp	(-)Ip,ax10 ⁶ mAmp	Ip,cx10 ⁶ mAmp			
0.2662	0.1423	0.4086	77.1	2.77	0.4202	0.0619	2.73
0.2670	0.1072	0.3743	69.9	5.52	0.5639	0.0799	5.52
0.2305	0.0828	0.3134	55.2	8.26	0.4929	0.0738	8.26
0.2291	0.0721	0.3013	54.9	11.0	0.4854	0.0784	11.0
0.2213	0.0524	0.2738	56.8	13.7	0.5487	0.0844	13.7

Dax1 ⁵ cm ² .s ⁻¹	Dcx10 ⁵ cm ² .s ⁻¹	E _{pc/2}	E _{pa} -E _{pc/2}	αna	k _{sc} x10 ²	Γ _{cx} x10 ⁹ mol/cm	(+)Q _c x10 ⁵ coulomb	Γ _{ax} x10 ⁹ mol/cm	(-)Q _{ax} x10 ⁵ coulomb
1.5418	1.72E	0.0615	0.0808	0.5763	1.49	1.5193	9.21	6.3849	3.87
1.2687	7.88	0.0340	0.0732	0.6359	5.35	1.0269	6.22	5.7920	3.51
7.8951	3.25	0.0210	0.0617	0.7539	3.52	9.2681	5.62	4.5690	2.77
7.8216	3.33	0.0166	0.0554	0.8394	2.95	9.3685	5.68	4.5476	2.76
8.3766	2.79	0.0088	0.0436	1.0674	1.76	8.5767	5.20	4.7062	2.85

The catalytic oxygen reduction wave at -1.0 V is decreased by an increase in crystal violet concentration explaining the decrease in catalytic decomposition of water using crystal violet.

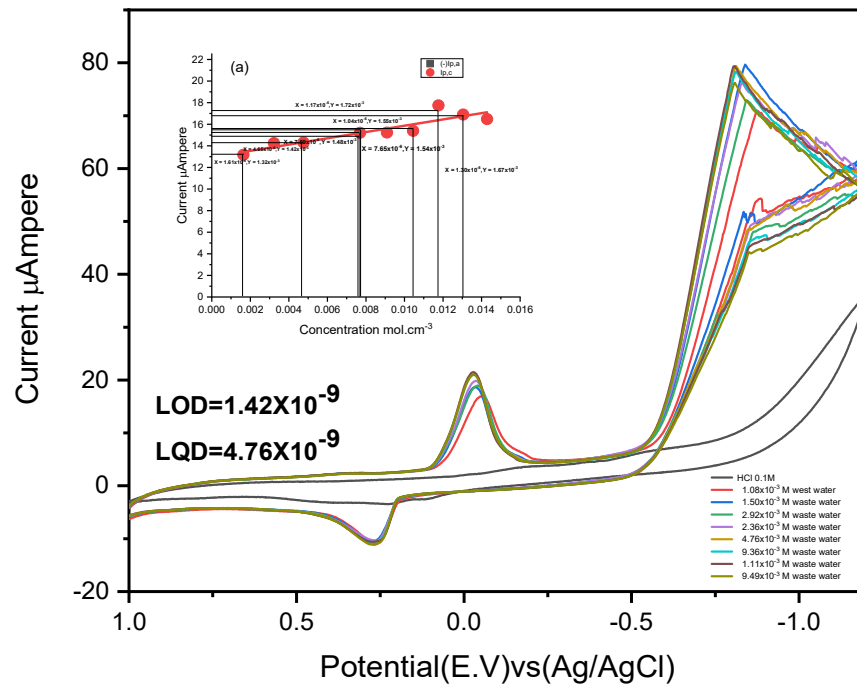


Figure 4. Wastewater calcium ion concentrations (in HCl, 0.1 V/s and 291.15 K). (a) Relation between (I_p, a) versus calcium ion concentrations.

Analysis of calcium quantity in Mansoura wastewater

The calcium ion determination was done for a sample getting from wastewater in the Mansoura city area and the sample was purified and then analyzed analytical data for calcium ions were done following the standard curve given in Figure 4. Which illustrated data given in and Table 3. The concentration of calcium ions in the wastewater was determined by the atomic absorption spectrophotometer the value was 6 ppm [33-35].

Table 3. Calcium ion parameters for waste water (in HCl, 0.1 V/s and 291.15 K).

[M] x10 ⁵ mol.L ⁻¹	Volt			Amp		Ip,a/Ip,c	Volt	R ²
	(-) Ep,a	Ep,c	ΔEp	(-)Ip,ax10 ⁶ mAmp	Ip,cx10 ⁶ mAmp		E°	
1.08	0.2324	0.0426	0.2750	55.0	13.2	0.4176	0.0948	0.9977
1.50	0.2645	0.0202	0.2848	73.9	15.4	0.4789	0.1221	0.9735
2.92	0.2635	0.0365	0.3000	77.8	14.8	0.5261	0.1135	0.9723
2.36	0.2491	0.0104	0.2595	71.7	14.2	0.5040	0.1193	0.9712
4.76	0.2568	0.0058	0.2626	76.1	15.3	0.4975	0.1254	0.9733
9.36	0.2557	0.0173	0.2731	79.5	17.2	0.4621	0.1191	0.9762
11.1	0.2537	0.0126	0.2664	76.4	16.6	0.4612	0.1205	0.9753
11.49	0.2528	0.0056	0.2584	80.5	15.6	0.5162	0.1235	0.9738

Dax10 ⁵ cm ² .S ⁻¹	Dcx10 ⁵ cm ² .S ⁻¹	Epc/2	Epa- Epc/2	α _{na}	k _{sc} x10 ²	Γcx10 ⁹ mol.cm ⁻²	(+)Qcx10 ⁵ coulomb	Γax10 ⁹ mol.cm ⁻²	(-)Qax10 ⁵ coulomb
49.55	5.04	0.0049	0.0475	0.9794	7.35	1.0907	6.61	4.555	2.76
41.54	3.58	0.0272	0.0475	0.9802	7.52	1.2784	7.75	6.1232	3.71
12.18	8.69	0.0192	0.0557	0.8350	4.64	1.2248	7.42	6.4447	3.91
15.81	1.23	5.13	0.0103	4.5012	5.71	1.1779	7.14	5.9368	3.60
4.377	3.49	0.0283	0.0341	1.3622	1.78	1.2673	7.68	6.3053	3.82
1.2348	1.14	0.0288	0.0462	1.0069	1.08	1.4246	8.63	6.5839	3.99
0.8070	7.49	0.0279	0.0406	1.1473	8.16	1.3714	8.31	6.3254	3.83
1.2316	9.13	0.0213	0.0269	1.7289	9.43	1.2917	7.83	6.6688	4.04

R² has good values indicating that the estimation procedure given is acceptable one.

Analysis of calcium in Mansoura wastewater by using crystal violet

Figure 5 results can be used for catalytic production of O₂ from wastewater as an environmental application. On adding crystal violet to the filtered wastewater of Mansoura City in Egypt, the calcium ion can be estimated following the standard curve for crystal violet as explained in Figure 5.

Anti-bacterial effect on calcium complex with crystal violet and face mask N-95 tissue

Microbial susceptibility testing. Filter paper disc assay: The antimicrobial activity of samples was estimated by disc diffusion method using inoculums containing 10⁶ bacterial spread on Mueller Hinton agar plates [36]. The sample discs were placed on the surface of agar plates seeded with the test organisms. The plates were incubated at 37 °C. Diameters of the inhibition zone (mm) were measured after 18-24 hours for bacteria.

Tested bacterial strains. Tested bacterial strains were *Bacillus cereus* and *E. coli*. The results are given in Table 4.

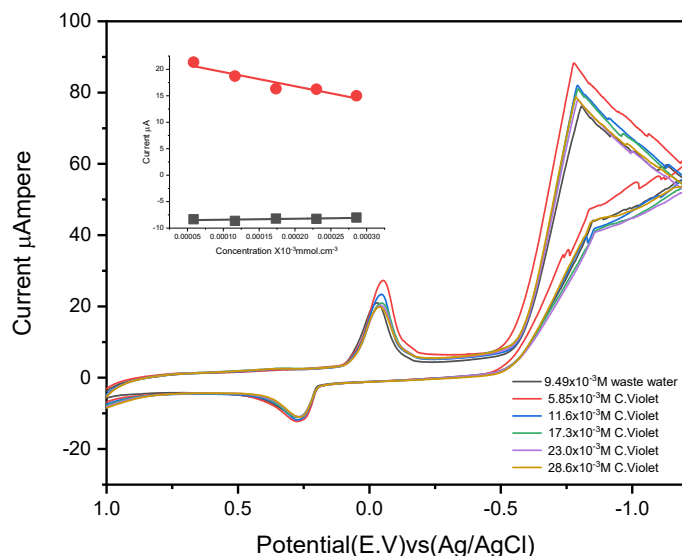


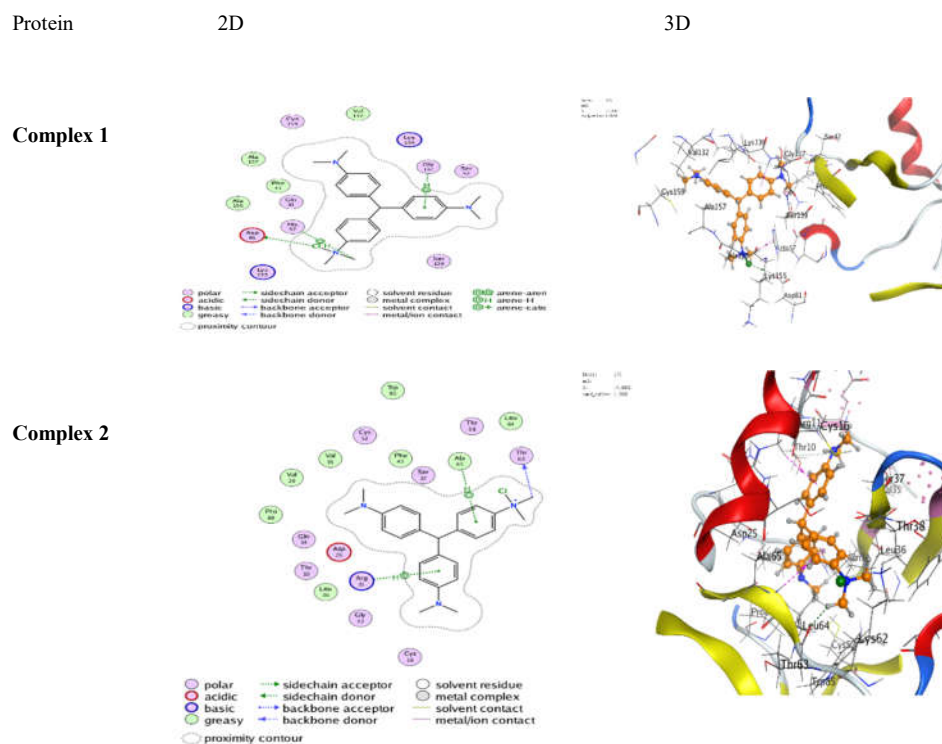
Figure 5. Cyclic voltammogram of the interaction of ($9.49 \times 10^{-3} \text{ M Ca}^{2+}$) of wastewater @ different concentrations of crystal violet (0.1 V/s and 291.15 K).

Table 4. Results of bacteria *Bacillus cereus* and *E. coli* in calcium ions with Crystal Violet in N-95 face mask tissue at 37 °C.

Samples	Tested organisms	
	<i>Bacillus cereus</i>	<i>E. coli</i>
1 (Ca+crystal)	18.3mm(14*12mm)	17.5mm (13*13)
2 (Ca+crystal+N95)	20mm(12*13mm)	-
3 (Ca+Dithizone)	15.6mm(13*13mm)	-
4 (Crystalviolet+N95)	25mm(16*13mm)	19mm(13*17mm)

The *bacillus cereus* was done and found that they have the explaining data in Table 4 with a big effect of crystal violet in the N-95 face mask advancing the addition of crystal violet to mask tissue to prevent bacteria to penetrate the tissue and capture it. Calcium + crystal violet are good also for interaction with *Bacillus cereus*. *E. coli* captured will be by using crystal violet on the use of an N-95 face mask.

Table 5. Crystal violet for the Interaction ligand- Calcium ions complexes with viral proteins (4i33, 4 KTC).



Molecular docking of crystal violet- Ca^{2+} with viral Hepatitis C virus protein (4i33, 4KTC)

Docking fits a ligand or complex into its target site by combining hydrophobic and electrostatic interactions. Table 5 illustrates the metal complexes that displayed Ca-crystal violet effects upon viral proteins (4i33, 4KTC) activated by Hepatitis C virus. Therefore, we docked the metal complexes toward these proteins, which were used for both viral proteins (4i33 and 4KTC). Complex 1 referred to the interaction of Ca-crystal violet with the first protein and complex 2 referred to the interaction of Ca-crystal violet with protein 2. This was done to study the posing and determining scoring binding sites. The higher negative binding energy indicates chelation. The docking ligating values for the complexes against viral proteins (4i33 and 4KTC) were -0.6, -0.9, -0.8, and -0.5, -0.9, -0.7 kcal/mol for complexes 1 and 2 [37, 38].

The potential interaction between viral proteins and the crystal violet- Ca^{2+} complex can be investigated via molecular docking. Size, spacing, number of poses, and scoring functions, all docking parameters show good interaction with the virus used in this study. The stability and energy of the dye complex-protein interaction are shown by the binding free energy calculation. In order to help in the development of new antiviral medicines or to better understand the mechanism of action of currently available dye complexes against Hepatitis C, molecular docking can provide useful information regarding potential interactions between dye complexes and Hepatitis C viral proteins.

CONCLUSION

In this study, which is a follow-up to earlier research, calcium ions can be estimated. For every concentration of calcium ions, sharp peaks are created, and as the concentration of calcium ions rises, so do the peaks' strengths. The total calcium ions for various environmental samples can be calculated using cyclic voltammetry and atom absorption spectroscopy. It is crucial for future research to employ sensors in the manner described in earlier work. Calcium interactions can be well-indicated utilizing techniques like calcium detection in water samples using cyclic voltammetry. The research on the *Bacillus cereus* revealed that the crystal violet added to the N-95 face mask advanced the goal of preventing germs from entering the tissue and engulfing it. *Bacillus cereus* interacts well when calcium and crystal violet are combined. Using a crystal violet face mask and an N-95 face shield, *E. coli* can be collected.

REFERANCES

1. Forney, L.J.; Reddy, C.A.; Tien, M.; Aust, S.D. The involvement of hydroxyl radical derived from hydrogen peroxide in lignin degradation by the white rot fungus *Phanerochaete Chrysosporium*. *J. Biol. Chem.* **1982**, *257*, 11455–11462.
2. Gomaa, E.A.; El-Defrawy, M.M.; Hussien, S.Q. Estimation of cyclic voltammetry data for SrCl₂, CaCl₂ and their interaction with ceftriaxone sodium salt in KNO₃ using palladium working electrode. *Eur. J. Adv. Chem. Res.* **2020**, *1*. DOI: 10.24018/ejchem.2020.1.5.18.
3. Fakayode, O.J. Nkambule, T.T.I. Cyclic voltammetric determination of calcium in water in the presence of natural organic matter (humic acid) and Cu(II) at gold electrode's surface. *Food Chem. Adv.* **2022**, *1*, 100012. <https://doi.org/10.1016/j.focha.2022.100012>.
4. Yu, J.; Zeng, T.; Wang, H.; Zhang, H.; Sun, Y.; Chen, L.; Song, S.; Li, L.; Shi, H. Oxygen-defective MnO_{2-x} rattle-type microspheres mediated singlet oxygen oxidation of organics by peroxymonosulfate activation. *Chem. Eng. J.* **2020**, *394*, 124458.
5. Sale, M.V.; Reid, L.B.; Cocchi, L.; Pagnozzi, A.M.; Rose, S.E.; Mattingley, J.B. Brain changes following four weeks of unimanual motor training: Evidence from behavior, neural stimulation, cortical thickness, and functional MRI, Hum. *Brain Mapp.* **2017**, *38*, 4773–4787.
6. Moore, E.W. Ionized calcium in normal serum, ultrafiltrates, and whole blood determined by ion-exchange electrodes. *J. Clin. Invest.* **1970**, *49*, 318–334.
7. Gomaa, E.A.; Morsi, M.A.; Negm, A.E.; Sherif, Y.A. Cyclic voltammetry of bulk and nano manganese sulfate with doxorubicin using glassy carbon electrode. *Int. J. Nano Dimens.* **2017**, *8*, 89.
8. Badulla, W.F.S.; Hussein, W.A.A.; Arli, G. Study of electrochemical behavior of two chemically similar acridines: Tacrine and 9-aminoacridine on hanging mercury drop electrode. *Bull. Chem. Soc. Ethiop.* **2021**, *35*, 639–646.
9. Hussein, S.Q.; El-Defrawy, M.M.; Gomaa, E.A.; El-Ghalban, M.G. Analytical electrochemical sensing of calcium ions in HCl media in the presence of a dithizone ligand with its biological applications. *Int. J. Electrochem. Sci.* **2023**, *18*, 100249.
10. Abd El-Hady, M.N.; Gomaa, E.A.; Al-Harazie, A.G. Cyclic voltammetry of bulk and nano CdCl₂ with ceftazidime drug and some DFT calculations. *J. Mol. Liq.* **2019**, *276*, 970–985.
11. Mabbott, G.A. An introduction to cyclic voltammetry. *J. Chem. Educ.* **1983**, *60*, 697.
12. Tokman, N. The use of slurry sampling for the determination of manganese and copper in various samples by electrothermal atomic absorption spectrometry. *J. Hazard. Mater.* **2007**, *143*, 87–94.
13. Nadeau, K.; Mester, Z.; Yang, L. The direct and accurate determination of major elements Ca, K, Mg and Na in water by HR-ICPMS. *Sci. Rep.* **2018**, *8*, 1–6.
14. Kowalik, R. The voltammetric analysis of selenium electrodeposition from H₂SeO₃ solution on gold electrode. *Arch. Metall. Mater.* **2015**, *60*, 57–63.

15. Gomaa, E.A.; EL-Sonbati, A.Z.; Diab, M.A.; EL-Ghareib, M.S.; Salama, H.M. Cyclic voltammetry, kinetics, thermodynamic and molecular docking parameters for the interaction of nickel chloride with diphenylthiocarbazone. *Open Acad. J. Adv. Sci. Technol.* **2020**, *4*, 30–44.
16. Othman, M.A.F.; Othman, A.A.; Zuki, H.M. Dithizone modified silver electrode for the determination of metal ions in aqueous solution. *Malaysian J. Anal. Sci.* **2016**, *20*, 197–204.
17. Birghila, S.; Bratu, M.M.; Prajitura, C.; Roncea, F.N.; Negreanu-Pirjol, T. Spectrophotometric method for the determination of total proteins in egg white samples. *Rev. Chim. (Bucharest)* **2015**, *66*, 378–381.
18. Durmishi, B.H.; Ismaili, M.; Shabani, A.; Jusufi, S.; Fejzuli, X.; Kostovska, M.; Abduli, S. The physical, physical-chemical and chemical parameters determination of river water Shkumbini (Pena) (Part A). *Ohrid, Repub. Maced.* **2008**, *27*, 1–11.
19. Olajire, A.A.; Imeokparia, F.E. Water quality assessment of Osun River: Studies on inorganic nutrients. *Environ. Monit. Assess.* **2001**, *69*, 17–28.
20. Gruden, R.; Buchholz, A.; Kanoun, O. Electrochemical analysis of water and suds by impedance spectroscopy and cyclic voltammetry. *J. Sensors Sens. Syst.* **2014**, *3*, 133–140.
21. Fathi, M.; Gomaa, E.A.; Salem, S.E.; Killa, H.M.; Gouda, A.A.; Farouk, A.H. Parameters for the conductometric association for lump and nano $\text{CoSO}_4 \cdot 7\text{H}_2\text{O}$ in the presence and absence of fuchsin acid in water at different temperature. *Bull. Chem. Soc. Ethiop.* **2023**, *37*, 789–804.
22. Mohamed, A.; Yousef, S.; Nasser, W.S.; Osman, T.A.; Knebel, A.; Sánchez, E.P.V.; Hashem, T. Rapid photocatalytic degradation of phenol from water using composite nanofibers under UV. *Environ. Sci. Eur.* **2020**, *32*, 1–8.
23. El-Kot, D.A.; Gomaa, E.A.; El-askalany, A.M.H.; Zaky, R.R.; Abd El-Hady, M.N. Design of a novel-NOON-tetradentate Schiff-base scaffold supported by α -tetralone and benzothiazole moieties with its Cu^{2+} , Co^{2+} , and Cd^{2+} chelates. *J. Mol. Struct.* **2023**, 1278, 134901.
24. Sivashankar, N.; Thanigaivelan, R.; Saravanan, K.G. Electrochemical micromachining and parameter optimization on AZ31 alloy—ANN and TOPSIS techniques. *Bull. Chem. Soc. Ethiop.* **2023**, *37*, 1263–1273.
25. Ye, H.; Crooks, R.M. Electrocatalytic O_2 reduction at glassy carbon electrodes modified with dendrimer-encapsulated Pt nanoparticles. *J. Am. Chem. Soc.* **2005**, *127*, 4930–4934.
26. Almeida, J.M.S.; Dornellas, R.M.; Yotsumoto-Neto, S.; Ghisi, M.; Furtado, J.G.C.; Marques, E.P.; Aucélio, R.Q.; Marques, A.L.B. A simple electroanalytical procedure for the determination of calcium in biodiesel. *Fuel.* **2014**, *115*, 658–665.
27. Gomaa, E.A.; Tahoon, M.A.; Negm, A. Aqueous micro-solvation of Li^+ ions: Thermodynamics and energetic studies of $\text{Li}^+(\text{H}_2\text{O})_n$ ($n = 1-6$) structures. *J. Mol. Liq.* **2017**, *241*, 595–602.
28. Gomaa, E.A.; Zaky, R.R.; Shokr, A. Estimated the physical parameters of lanthanum chloride in water-N,N-dimethyl formamide mixtures using different techniques. *J. Mol. Liq.* **2017**, *242*, 913–918.
29. Gomaa, E.A.; Mahmoud, M.H.; Mousa, M.G.; El-Dahshan, E.M. Cyclic voltammetry for the interaction between bismuth nitrate and methyl red in potassium nitrate solutions. *Chem. Methodol.* **2018**, *3*, 1–11.
30. Nakanishi, J.; Kuramoto, I.; Baba, J.; Ogawa, K.; Yoshikawa, Y.; Ishiguro, H. Continuous hospitality with social robots at a hotel. *SN Appl. Sci.* **2020**, *2*, 1–13.
31. Murray, M.D.; Loos, B.; Tu, W.; Eckert, G.J.; Zhou, X.-H.; Tierney, W.M. Effects of computer-based prescribing on pharmacist work patterns. *J. Am. Med. Informatics Assoc.* **1998**, *5*, 546–553.
32. Daud, N.; Yusof, N.A.; Nor, S.M.M. Electrochemical characteristic of biotinyl somatostatin-14/Nafion modified gold electrode in development of sensor for determination of Hg(II) . *Int.*

- J. Electrochem. Sci.* **2013**, 8, 10086–10099.
33. AbouElleef, E.M.; Abd El-Hady, M.N.; Gomaa, E.A.; Al-Harazie, A.G. Conductometric association parameters for CdBr_2 in the presence and absence of ceftazidime in water and 30% ethanol-water mixtures. *J. Chem. Eng. Data* **2021**, 66, 878–889.
 34. Kayali, D.; Shama, N.A.; Aşır, S.; Dimililer, K. Machine learning based-models for the qualitative classification of potassium ferrocyanide using electrochemical methods. *J Supercomput.* **2023**, 79, 12472-12491.
 35. Rossotti, F.; Rossotti, H. *The Determination of Stability Constants and Other Equilibrium Constants in Solution*, 4th ed., McGraw-Hill Book Company Inc.: New York; **1961**.
 36. El-Baz, A.F.; Abbas, H.M. Isolation and identification of an endophytic fungus from ficus elastica decora and investigation of the antioxidant and antifungal bioactivities of its fermentation extract. *Menoufia J. Agric. Biotechnol.* **2017**, 2, 81–85.
 37. Sharfalddin, A.A.; Emwas, A.-H.; Jaremko, M.; Hussien, M.A. Synthesis and theoretical calculations of metal-antibiotic chelation with thiamphenicol: in vitro DNA and HSA binding, molecular docking, and cytotoxicity studies. *New J. Chem.* **2021**, 45, 9598–9613.
 38. Babgi, B.A.; Alzaidi, N.A.; Alsayari, J.H.; Emwas, A.-H.M.; Jaremko, M.; Abdellattif, M.H.; Aljahdali, M.; Hussien, M.A. Synthesis, HSA-binding and anticancer properties of $[\text{Cu}^2(\mu\text{-dppm})_2(\text{N}^{\wedge}\text{N})_2]^{2+}$. *J. Inorg. Organomet. Polym. Mater.* **2022**, 32, 4005–4013.